Journal of Hepatocellular Carcinoma

Dovepress
Taylor & Francis Group

Open Access Full Text Article

ORIGINAL RESEARCH

Prognostic Value of Tumor Immune Microenvironment and Peripheral Blood Inflammatory Cells in Hepatocellular Carcinoma

Lin Sun[1,*], Zhensheng Yue[1,2,*], Lin Wang[1]

[1]Department of Hepatobiliary Surgery, Xi-Jing Hospital, Fourth Military Medical University, Xi'an, 710032, People's Republic of China; [2]Department of Ophthalmology, Xi-Jing Hospital, Fourth Military Medical University, Xi'an, People's Republic of China

*These authors contributed equally to this work

Correspondence: Lin Wang, Department of Hepatobiliary Surgery, Xijing Hospital, Fourth Military Medical University, Xi'an, People's Republic of China, Tel +86-29-84775933, Fax +86-29-83246270, Email 1749771520@qq.com

Background: The tumor immune microenvironment and ratios of peripheral blood inflammatory factors have been associated with prognosis in various malignancies. While they show prognostic potential in some cancers, their value in hepatocellular carcinoma (HCC) remains unclear.

Methods: We analyzed 371 HCC patients from The Cancer Genome Atlas (TCGA) and a retrospective cohort from Xijing Hospital. Optimal cut-off values for the lymphocyte-to-monocyte ratio (LMR), prognostic nutritional index (PNI), and platelet-to-lymphocyte ratio (PLR) were determined using ROC curve analysis. Associations with clinicopathological features and disease-free survival (DFS) were assessed using Kaplan-Meier and Cox regression analyses.

Results: Kaplan-Meier analysis showed that high CD8+ T cell and NK cell infiltration were associated with favorable outcomes. Univariate analysis identified low PNI (≤41.6), low LMR (≤2.38), high PLR (>88.64), age, and lymph node metastasis as significant risk factors for DFS. Multivariate Cox analysis established low PNI, high PLR, and lymph node metastasis as independent prognostic factors.

Conclusion: High intratumoral CD8+ T cell and natural killer cell (NK cell) levels correlate with better survival. Preoperative PNI, PLR, and lymph node status are independent prognostic indicators for HCC patients.

Keywords: peripheral blood inflammatory markers, clinicopathological features, hepatocellular carcinoma, prognosis

Introduction

Hepatocellular carcinoma (HCC) remains a major cause of cancer-related death worldwide, with high incidence and poor survival rates.[1] Its development is a multi-step process arising from chronic liver injury, with established risk factors including chronic hepatitis B (HBV) or C (HCV) infection, excessive alcohol consumption, non-alcoholic steatohepatitis (NASH), and dietary aflatoxin exposure.[2] Despite this diversity, most HCC cases share a common pathophysiological basis: sustained chronic inflammation.

Chronic inflammation is a key driver of hepatocarcinogenesis, fostering a microenvironment conducive to tumor initiation and progression. Repeated liver injury activates resident immune cells such as Kupffer cells and hepatic stellate cells, leading to prolonged release of pro-inflammatory cytokines, chemokines, and growth factors.[3] This inflammatory environment promotes ongoing cell proliferation, tissue repair, and angiogenesis. Combined with accumulating genomic instability, it significantly raises the risk of malignant transformation, establishing inflammation as a central oncogenic driver rather than a bystander.[4]

The Tumor Immune Microenvironment (TIME) is essential to understanding HCC biology. TIME consists of a complex network of immune cells, stromal components, signaling molecules, and extracellular matrix that collectively influence tumor behavior and treatment response.[5] HCC TIME is highly heterogeneous, ranging from immune-rich

https://doi.org/10.2147/JHC.S587532
Received: 16 December 2025
Accepted: 10 April 2026
Published: 20 April 2026

("hot") to immune-deficient ("cold") phenotypes, each linked to distinct clinical outcomes.[6] Key cellular components include anti-tumor CD8+ T cells; immunosuppressive myeloid-derived suppressor cells (MDSCs) and tumor-associated macrophages (TAMs); and regulatory T cells (Tregs) that further suppress immune responses.[7] The balance among these elements determines whether immunity controls or facilitates tumor progression.

The discovery of regulatory T cells (Tregs) and their master transcription factor FOXP3, which was honored by the 2025 Nobel Prize in Physiology or Medicine, has fundamentally advanced our understanding of immune tolerance and opened new avenues for immunotherapy.[8] This paradigm offers new insights into HCC pathogenesis: chronic liver injury may epigenetically reprogram Kupffer cells and other innate immune cells into a persistently activated, "trained" state, thereby sustaining the pro-inflammatory milieu that drives carcinogenesis and shapes an immunosuppressive TIME. This mechanism also helps explain the systemic inflammatory response in HCC patients, suggesting that peripheral immune markers may reflect underlying "trained immunity" processes.

Systemic inflammation, reflected in peripheral blood, provides complementary and readily accessible prognostic information. Elevated levels of circulating cytokines such as IL-6 and TNF-α are consistently associated with HCC risk, disease stage, and survival.[9,10] Additionally, composite indices derived from routine blood counts—including the neutrophil-to-lymphocyte ratio (NLR), platelet-to-lymphocyte ratio (PLR), lymphocyte-to-monocyte ratio (LMR), and prognostic nutritional index (PNI)—have proven to be cost-effective tools for predicting survival and recurrence in HCC patients.[11,12] A critical unanswered question remains how these systemic inflammatory markers relate to and reflect the complex local immune landscape of the TIME.

Therefore, this study aims to bridge these two critical dimensions by integrating an analysis of the local TIME with an evaluation of systemic inflammatory markers. We hypothesize that the systemic inflammatory state, as captured by peripheral blood indices, mirrors specific immune configurations within the tumor microenvironment, and that their combined assessment offers superior prognostic value. Such an integrated approach is paramount for deepening our understanding of HCC immunobiology and holds significant promise for refining risk stratification, improving prognostic accuracy, and guiding the development of novel immunotherapeutic strategies.

Materials and Methods

Patient Cohorts and Data Collection

This study utilized data from two distinct cohorts. First, Clinical data on tumor immune infiltration and prognosis were obtained from a cohort of 371 Hepatocellular Carcinoma (HCC) patients in The Cancer Genome Atlas (TCGA). We have uploaded the patient information from the TCGA database (Supplementary Material). RNA-seq expression data (FPKM) were downloaded from TCGA, converted to TPM, and log2-transformed. Immune infiltration scores were calculated using the CIBERSORT algorithm with the LM22 gene signature, and only samples with $P < 0.05$ were retained. Data preprocessing included conversion of FPKM to TPM, log2 transformation, and removal of low-expression genes. Feature selection was performed using univariate Cox regression to identify immune cell types associated with survival. Second, a retrospective analysis was conducted on an internal cohort from Xijing Hospital, Air Force Medical University. This study was approved by the hospital's Ethics Committee and adhered to the principles of the Declaration of Helsinki. The Ethics Committee granted a waiver for informed consent. We initially screened 98 patients diagnosed with HCC between January 1, 2020, and December 31, 2022. The inclusion criteria were: (a) surgical resection for HCC at our hospital with postoperative pathological confirmation; (b) no neoadjuvant therapy prior to surgery; (c) complete pathological records and peripheral blood cell counts; (d) absence of active infection or hematological diseases; and (e) a postoperative disease-free survival (DFS) exceeding 6 months. Exclusion criteria included: (a) preoperative use of medications known to affect blood counts; (b) a history of other concurrent malignancies; (c) failure to adhere to standard postoperative treatment regimens; and (d) presence of other severe underlying medical conditions. Peripheral blood parameters, including absolute lymphocyte (L), neutrophil (N), and platelet (P) counts, as well as serum albumin levels, were collected from medical records. The Prognostic Nutritional Index (PNI) was calculated using the formula: $10 \times$ serum albumin value (g/dL) $+ 0.005 \times$ peripheral lymphocyte count (per mm^3). Clinicopathological characteristics, such as

lymph node status, age, and the presence of vascular tumor thrombus, were also collected. All hematological indices were within normal ranges at the time of measurement.

Follow-Up

Patients from the internal cohort were followed every 3 months for the first 3 years postoperatively and every 6 months thereafter. Follow-up assessments included clinical and laboratory evaluations, liver magnetic resonance imaging (MRI), and other investigations as deemed clinically appropriate. Disease-free survival (DFS) was defined as the duration from the date of diagnosis to the date of disease recurrence, metastasis, or the last follow-up. The follow-up period concluded on September 1, 2025, with data collected through outpatient reviews and telephone interviews. The censoring rate for all followed patients was maintained below 20%.

Statistical Analysis

TCGA data were processed, analyzed, and visualized using R software (version 4.3.3) with packages including "ggplot2" and "ggpubr". ggplot2 was used to construct graphical objects and achieve data visualization through layered superimposition. All boxplots, scatter plots, and group comparison figures in this study were generated based on this package. ggpubr simplifies the process of adding statistical tests and annotations on the basis of ggplot2. Specifically, the stat_compare_means() function was employed to automatically calculate pairwise P-values and add significance labels directly to the graphs. Statistical analyses for the internal clinical cohort were performed using IBM SPSS Statistics (Version 24.0) and GraphPad Prism (Version 10.0.2). The two groups, High and Low, are dichotomized using the median: values > median are assigned to the High group, and values ≤ median are assigned to the Low group. A robustness check is performed: if the sample size of either group is < 5, the feature is skipped. Then, Kaplan-Meier and Log rank tests are conducted based on the grouping, and the Cox HR is calculated. Receiver Operating Characteristic (ROC) curve analysis was employed to determine the predictive ability and optimal cutoff values for LMR, PLR, and PNI. Survival curves were generated using the Kaplan-Meier method and compared with the Log rank test. Categorical variables were analyzed using the Chi-square test or Fisher's exact test. Univariate and multivariate analyses were conducted with the Cox proportional hazards regression model. All P-values were two-sided, and a value of less than 0.05 was considered statistically significant.

Reporting Guidelines

To ensure the transparency, reproducibility, and comprehensive reporting of this integrative study, we adhered to the following established reporting guidelines:

For the retrospective clinical cohort component, including patient enrollment, data collection, and survival analysis, we followed the Strengthening the Reporting of Observational Studies in Epidemiology (STROBE) statement.

Results

Prognostic Value of Immune Cell Infiltration in HCC Patients

Kaplan-Meier survival analysis revealed a significant impact of CD8+T cell infiltration levels on patient prognosis. The survival probability of the high-infiltration group was markedly superior to that of the low-infiltration group. The survival curves for these two groups began to diverge early in the follow-up period (approximately at 200 days, Figure 1A) and maintained a significant separation throughout. The estimated 5-year survival rate was approximately 45% for the high-infiltration group, compared to about 30% for the low-infiltration group. The Log rank test yielded a $P < 0.05$, confirming the statistical significance of this difference. Conversely, an elevated myeloid-to-lymphocyte ratio (MLR) was significantly associated with poorer prognosis. Although the P-value was 0.068, slightly above the conventional significance threshold of 0.05, a clear trend was observed (Figure 1B). Furthermore, the level of NK cell infiltration demonstrated a protective trend for patient survival. Patients in the high-NK group exhibited a markedly higher survival probability than those in the low-NK group, presenting a pattern opposite to that of effector immune cells (Figure 1C).

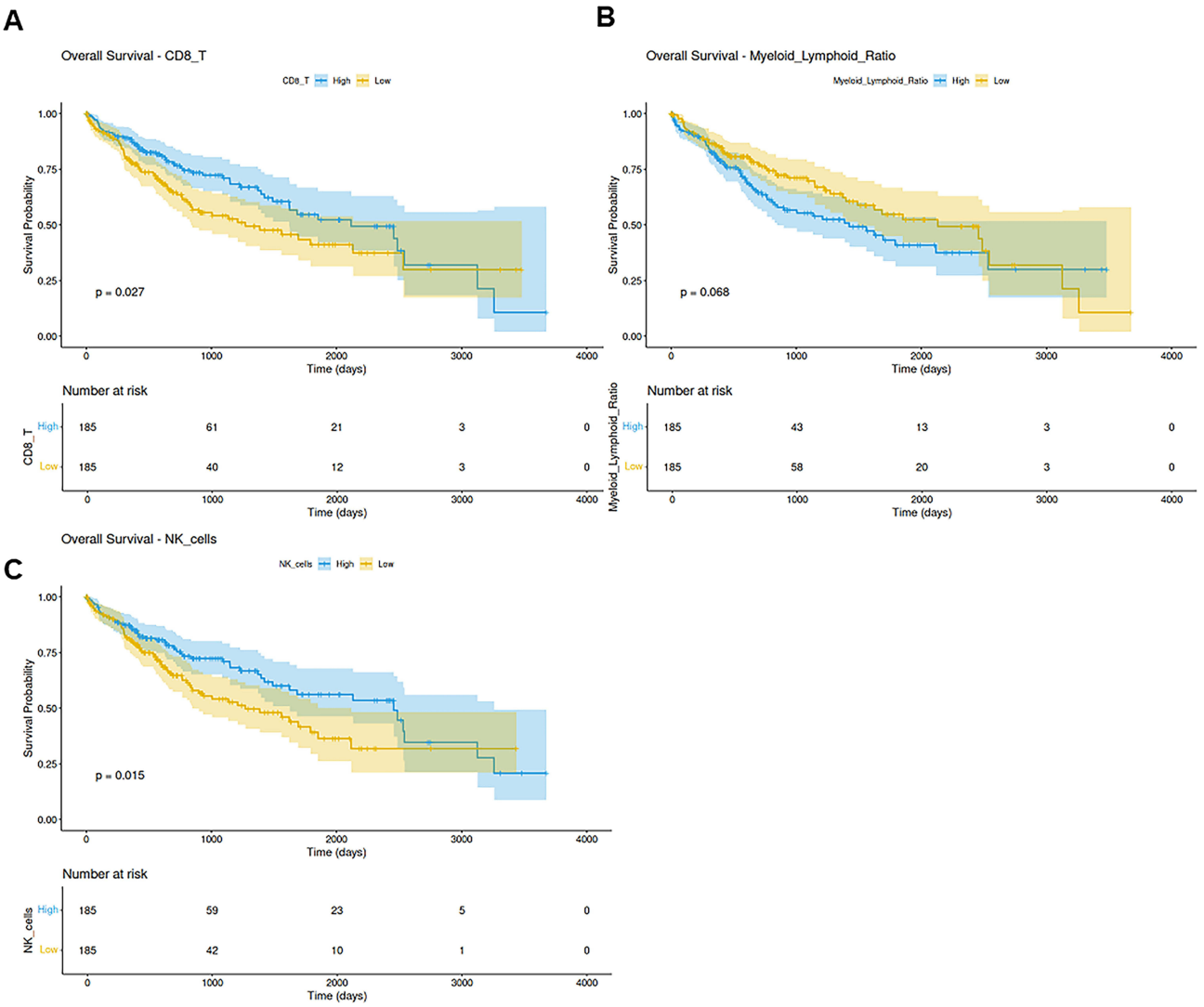

Figure 1 Kaplan-Meier survival analysis according to immune cell infiltration and systemic inflammatory ratio. (**A**) Patients with high CD8+ T cell infiltration exhibited significantly better overall survival compared to those with low infiltration (Log-rank P < 0.05). (**B**) Patients with a high myeloid-to-lymphocyte ratio (MLR) showed poorer overall survival (Log-rank P = 0.068). (**C**) Patients with high NK cell infiltration exhibited significantly better overall survival compared to those with low infiltration (Log-rank P < 0.05).

Interplay of Inflammatory Cells in the HCC Immune Microenvironment

A correlation heatmap was utilized to visualize the Spearman correlation coefficients among 13 distinct immune scores. The color intensity represents the strength of the correlation, with red indicating positive and blue indicating negative associations. Hierarchical clustering was applied to group immune features with similar patterns.The analysis revealed strong positive correlations ($r > 0.7$) between T_cells and HLA ($r = 0.81$), Cytokines and Chemokines ($r = 0.83$), and CD8+T and T_cells ($r = 0.87$), B_cells and T_cells ($r = 0.77$), NK_cells and CD8+T ($r = 0.88$), and Checkpoints and T_cells ($r = 0.89$). These findings reflect the dependency of antigen presentation on T cell activation, the coordinated action within inflammatory signaling networks, and the integral role of CD8+T cells within the overall T cell population, respectively. Moderate positive correlations ($0.4 < r < 0.7$) were observed between B_cells and HLA ($r = 0.66$), NK_cells and Chemokines ($r = 0.57$). These relationships suggest coordinated adaptive immunity, concordance in cytotoxic immune responses, and the balance between immune activation and negative regulation, respectively. Conversely, negative correlations were identified between the Myeloid_Lymphoid_Ratio and T_cells ($r = -0.45$), and between the Inflammatory_Index and NK_cells ($r = -0.50$, $r = -0.78$). These inverse relationships highlight the antagonism between myeloid cell infiltration and T cell presence, as well as the potential suppressive effect of a chronic inflammatory state on

NK cell function (Figure 2A). In summary, the results indicate a tendency for co-infiltration among effector immune cells (T, B, NK), while immunosuppressive features (eg., high MLR, inflammation) are negatively correlated with effector immunity. A circos plot provided an intuitive visualization of these relationships, where circle size corresponds to the absolute value of the correlation coefficient and color denotes the direction of the association (Figure 2B). The corresponding correlation matrix displaying the exact numerical values is also provided (Figure 2C).

Immune Infiltration Patterns in HCC Patients

We employed a heatmap to visualize the expression patterns of 13 immune features (rows) across 371 HCC samples (columns). Bidirectional hierarchical clustering was applied to reorder both samples and immune features, revealing intrinsic patterns within the tumor immune microenvironment (Figure 3A). Based on the clustering analysis, three distinct immune infiltration patterns were identified: Immune-Hot Tumors (approximately 30% of samples): This subtype

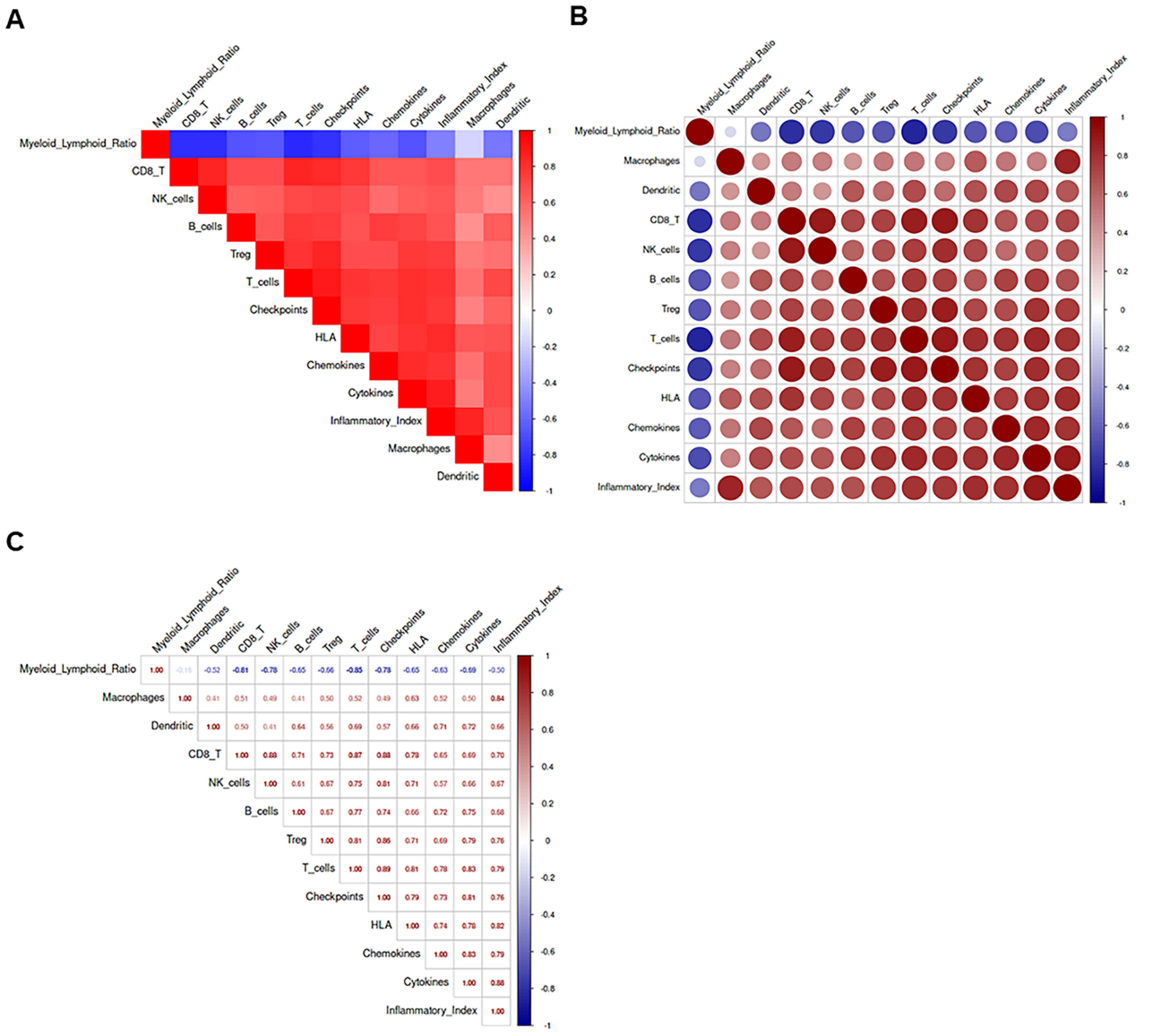

Figure 2 Analysis of interrelationships among tumor immune microenvironment features. (**A**) Heatmap of Spearman correlation coefficients among 13 immune scores. Hierarchical clustering was applied to both rows and columns. Red and blue colors represent positive and negative correlations, respectively. (**B**) Circos plot visualizing the significant correlations. The size of the circles represents the absolute value of the correlation coefficient, and the color indicates the direction (red: positive, blue: negative). (**C**) Correlation matrix displaying the exact numerical Spearman correlation coefficients for all pairwise comparisons.

https://doi.org/10.2147/JHC.S587532

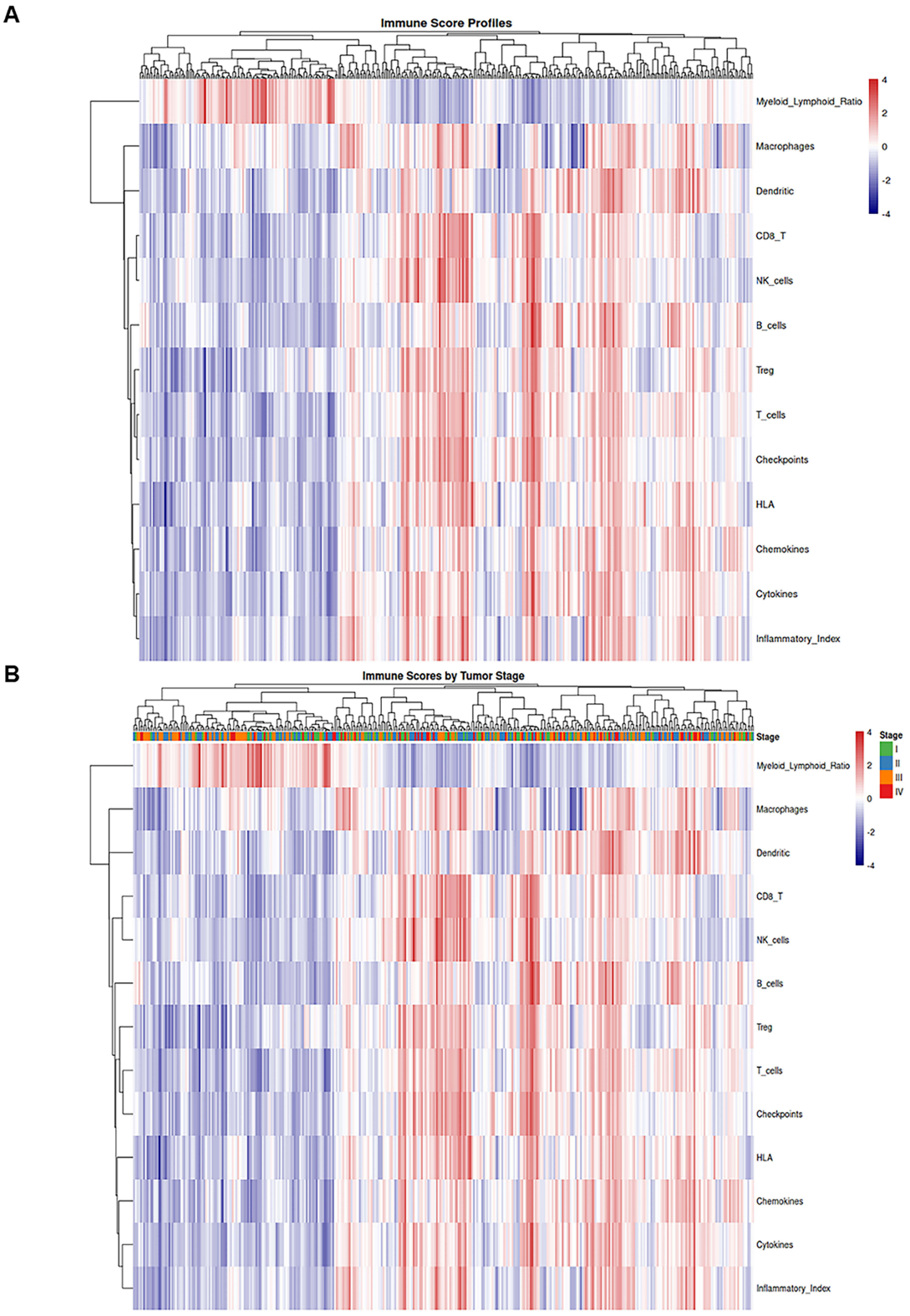

Figure 3 Immune landscape and its link to progression in HCC. (**A**) Clustering of 371 HCC samples based on 13 immune features identified three subtypes: Immune-Hot (30%), Immune-Cold (40%), and Myeloid-Dominated (30%). (**B**) Samples sorted by tumor stage (I–IV) show a progressive shift in the immune microenvironment, characterized by reduced effector immunity and elevated immunosuppressive signals in advanced stages.

https://doi.org/10.2147/JHC.S587532

was characterized by concurrent high infiltration of multiple immune cell types. It featured coordinated enrichment of T cells, B cells, and NK cells, accompanied by elevated expression of HLA molecules and immune checkpoint markers. Immune-Cold Tumors (approximately 40% of samples): This group exhibited an overall low level of immune infiltration, with a notable absence of effector immune cells, suggesting a phenotype typically associated with poor prognosis. Myeloid-Dominated Tumors (approximately 30% of samples): This pattern was defined by high Macrophage and Dendritic cell scores, coupled with relatively low lymphocyte infiltration. These tumors also displayed a high Myeloid-to-Lymphoid Ratio (MLR) and Inflammatory Index, potentially representing an immunosuppressive microenvironment. Subsequently, we investigated the correlation between immune infiltration and disease progression by sorting the 371 patients according to their tumor stage (Stages I–IV, Figure 3B). The results indicated that patients with Stage I–II disease maintained relatively high T cell and B cell infiltration, suggesting a more intact state of immune surveillance. In Stage III patients, the level of immune infiltration began to decline and exhibited greater heterogeneity. Finally, Stage IV patients demonstrated an overall reduction in immune infiltration alongside increased expression of immune checkpoints. This progressive shift across stages suggests the gradual establishment of tumor immune escape mechanisms as the disease advances.

Comparison of Immune Infiltration Across Different Disease Stages

To investigate the association between disease stage and immune cell infiltration in detail, we performed Kruskal–Wallis tests for each immune feature. The level of B-cell infiltration was significantly lower in the early stages (Stage I–II) than in the advanced stages (Stage III–IV) ($P < 0.05$), suggesting increased heterogeneity of B-cell infiltration in advanced tumors (Figure 4C).In contrast, there are not significant trend in T cell infiltration,CD8+ T cells, Checkpoints and NK cells with advancing disease stage ($P > 0.05$, Figure 4A–E).

Evaluation of Prognosis-Associated Markers

The top 10 immune features associated with prognosis are displayed in descending order of statistical significance (ie., arranged from the smallest to largest P-value). The bar height represents the -log10(P-value), with a greater height indicating stronger statistical significance. A red dashed line marks the significance threshold of $P = 0.05$. As shown in Figure 5A, NK cell infiltration, CD8+ T cell infiltration, and the Myeloid-to-Lymphocyte Ratio (MLR) ranked as the top three most significant and reliable prognostic markers. Figure 5B presents a forest plot summarizing the univariable Cox regression results for all immune features. The horizontal axis represents the hazard ratio (HR), with the vertical dashed line indicating HR=1 (the line of no effect). The point estimates and their 95% confidence intervals demonstrate the prognostic value of each feature. The accompanying Table 1 displays key statistical outcomes, including HR values and P-values for the immune features.

Baseline Characteristics of the Internal Validation Cohort

A total of 98 patients from our institution were ultimately enrolled in the study based on the predefined inclusion and exclusion criteria. The detailed baseline clinical and pathological characteristics of this cohort are summarized in Table 2.

Optimal Cutoff Values of PNI, LMR, and PLR for Prognostic Prediction

The area under the curve (AUC) for predicting disease-free survival (DFS) was 0.856 ($P < 0.001$) for PNI (Figure 6A), 0.714 ($P = 0.035$) for LMR (Figure 6B), and 0.709 ($P = 0.039$) for PLR (Figure 6C). The optimal pretreatment cutoff values were determined as 41.6 for PNI, 2.38 for LMR, and 88.64 for PLR. In contrast, NLR showed no significant prognostic value in this cohort (Figure 6D).

Association of PNI, LMR, and PLR with Prognosis in HCC Patients

Based on the optimal cutoff values, patients were categorized into two groups: low PNI (≤41.6, n = 25) and high PNI (>41.6, n = 73). Kaplan–Meier analysis showed that the high PNI group had a 3-year disease-free survival (DFS) rate of 98.6%, compared to 92.0% in the low PNI group, with a statistically significant difference ($P < 0.05$, Log rank test). Similarly, survival analysis for LMR revealed a 3-year DFS rate of 97.2% in the high LMR group and 96.3% in the low

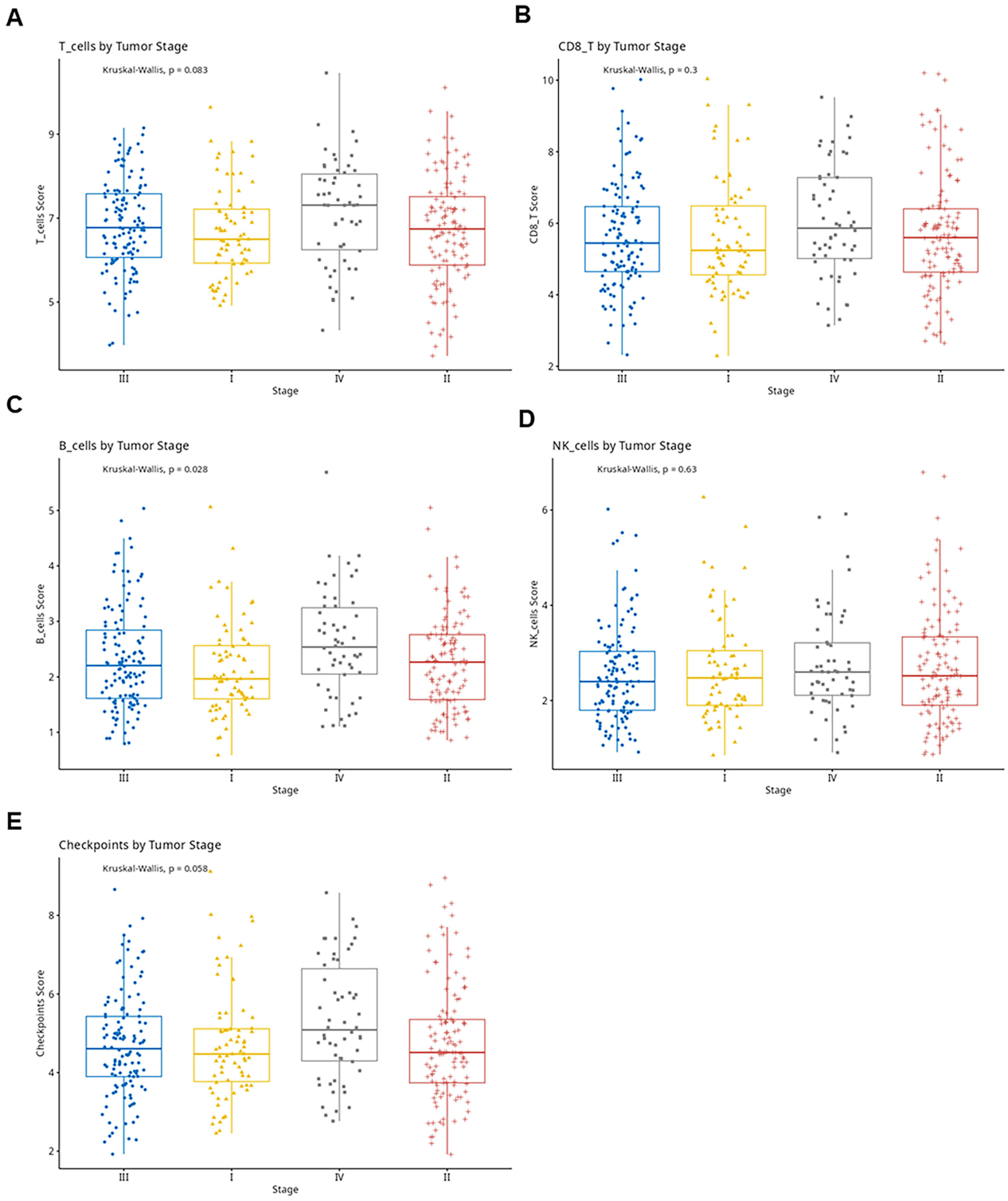

Figure 4 Association of key immune features with tumor stage in hepatocellular carcinoma. (**A**) T cell scores showed a no significant trend with advancing stage (P = 0.083). (**B**) CD8+ T cell showed a no significant trend with advancing stage (P = 0.30). (**C**) B cell infiltration showed a significant increasing trend across stages (P = 0.028). (**D**) NK cell scores remained stable in early stages but declined significantly in later stages (P = 0.63). (**E**) The expression of immune checkpoint molecules exhibited a trend with tumor stage, peaking in Stage IV (P = 0.058). Different colored boxplots represent tumor stages I–IV. Statistical analysis was performed using the Kruskal–Wallis test in the training set.

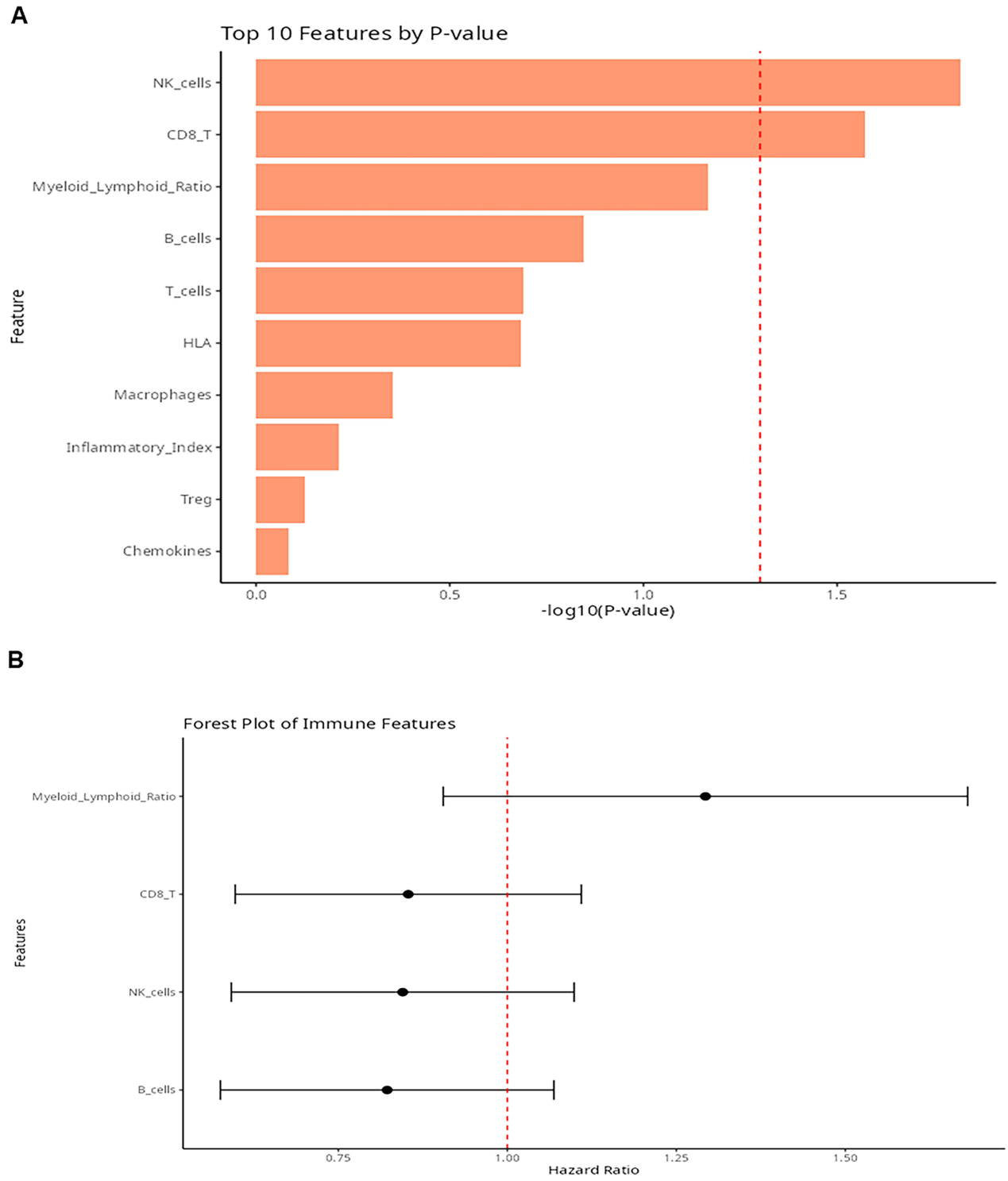

Figure 5 Ranking of top prognostic immune features (**A**) The top 10 immune features are ranked by their association with overall survival (-log10(P-value)). The red dashed line denotes P = 0.05. NK cells, CD8+ T cells, and MLR were the top three prognostic markers. (**B**) Forest plot summarizing univariable Cox regression analyses, illustrating the association between immune features and outcome. Hazard ratios (HR) with 95% confidence intervals are plotted relative to the no-effect line (HR=1).

https://doi.org/10.2147/JHC.S587532

Table 1 Key Statistical Outcomes, Including Hazard Ratios (HR) and P-values for the Immune Features

Feature	HR	P_value
NK_cells	0.845	0.0152
CD8_T	0.853	0.0267
Myeloid_Lymphoid_Ratio	1.293	0.0683
B_cells	0.822	0.1425
T_cells	0.913	0.2047
HLA	0.891	0.2078
Macrophages	0.891	0.4448
Inflammatory_Index	0.991	0.6133
Treg	0.976	0.7474
Chemokines	0.999	0.8240

Table 2 Baseline Characteristics of Patients with Hepatocellular Carcinoma

Clinicopathological Characteristics	Number (n=98)	Percentage (%)
Age (years)		
≤60	75	76.5
>60	23	23.5
Sex		
Male	82	83.7
Female	16	16.3
Lymphovascular Invasion (LVI)		
Negative	69	70.4
Positive	29	29.6
Lymph node status		
Negative	91	92.9
Positive	7	7.1

LMR group, which was not statistically significant ($P > 0.05$). For PLR, the high PLR group had a 3-year DFS of 95.5%, while the low PLR group reached 98.1%, showing a significant difference between groups ($P < 0.05$, Log rank test) (Figure 7A–C).

Univariate and Multivariate Analysis of PNI, LMR, PLR, and DFS

Univariate analysis indicated that PNI ($\chi^2 = 14.247$, $P < 0.001$), LMR ($\chi^2 = 7.596$, $P = 0.006$), PLR ($\chi^2 = 7.752$, $P = 0.005$), age ($\chi^2 = 6.189$, $P = 0.013$), and lymph node status ($\chi^2 = 10.249$, $P = 0.001$) were significantly associated with 3-year DFS (Table 3). Multivariate Cox regression analysis demonstrated that PNI ($P = 0.019$), PLR ($P = 0.001$), and lymph node status ($P = 0.015$) remained independent prognostic factors, whereas LMR was not statistically significant ($P = 0.377$) (Table 4).

Association of LMR, PLR, and PNI with Clinicopathological Features

Using the optimal cutoff values, patients were stratified into high and low groups for each marker: LMR > 2.38 (high) vs. ≤ 2.38 (low), PLR > 88.64 (high) vs. ≤ 88.64 (low), and PNI > 41.6 (high) vs. ≤ 41.6 (low). The analysis revealed no statistically significant associations between these groups and clinicopathological features, including age, gender, vascular invasion, or lymph node status (Tables 5–7).

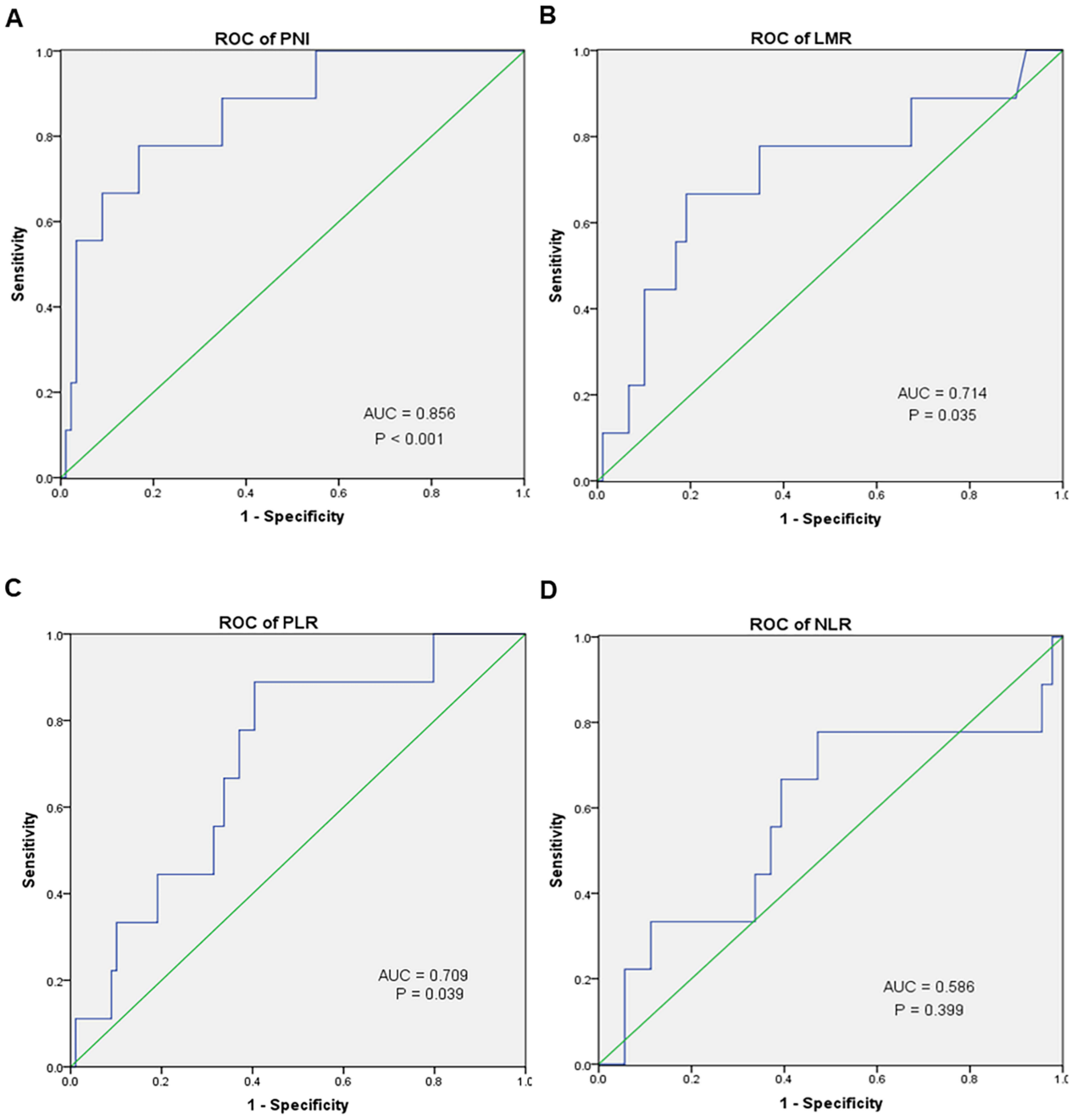

Figure 6 Receiver operating characteristic (ROC) curve analysis of systemic inflammatory markers for predicting disease-free survival (DFS). ROC curves evaluating the prognostic performance of (**A**) the Prognostic Nutritional Index (PNI), (**B**) the Lymphocyte-to-Monocyte Ratio (LMR), (**C**) the Platelet-to-Lymphocyte Ratio (PLR), and (**D**) the Neutrophil-to-Lymphocyte Ratio (NLR). The area under the curve (AUC), corresponding P-value, and the optimal pretreatment cutoff value for each marker are as follows: PNI (AUC = 0.856, P < 0.001, cutoff = 41.6), LMR (AUC = 0.714, P = 0.035, cutoff = 2.38), and PLR (AUC = 0.709, P = 0.039, cutoff = 88.64).

Discussion

This study provides a comprehensive analysis of the prognostic value of both the local tumor immune microenvironment (TIME) and systemic inflammatory markers in hepatocellular carcinoma (HCC). By integrating data from a public genomic cohort and a single-institution clinical cohort, our findings underscore that the interplay between localized immune cell infiltration and systemic host immune status is critical for determining clinical outcomes in HCC patients.

A principal finding of this work is the confirmation of CD8+ T cell infiltration as a robust favorable prognostic factor, a result aligning with the established cornerstone of cancer immunology that cytotoxic T lymphocytes are pivotal for anti-

https://doi.org/10.2147/JHC.S587532

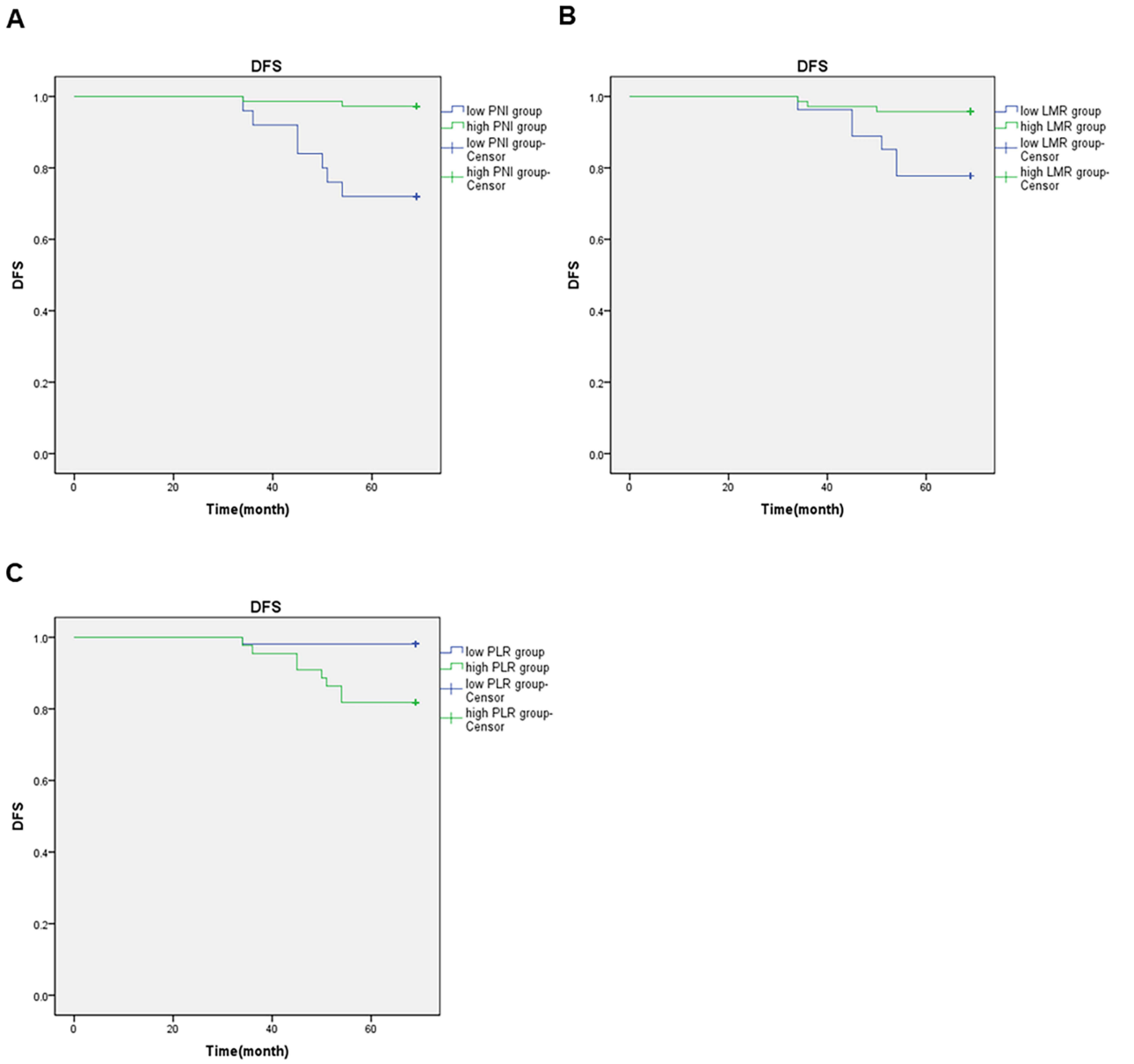

Figure 7 Disease-free survival stratified by inflammatory markers Kaplan-Meier curves compare DFS between patient groups stratified by optimal cutoffs. (**A**) PNI: High (>41.6) vs. Low (≤41.6) ($P < 0.05$). (**B**) LMR: High vs. Low ($P > 0.05$, NS). (**C**) PLR: Low vs. High ($P < 0.05$). The 3-year DFS rates are indicated for each group. NS, not significant.

tumor immunity. The observed positive correlations among T cells, B cells, and NK cells, coupled with their co-enrichment in the "immune-hot" cluster, delineate a coordinated adaptive immune network within the TIME. This suggests that effective anti-tumor immunity in HCC may rely on a collaborative effort between different lymphocyte lineages, rather than the function of a single cell type in isolation. In contrast, the prognostic value of myeloid- and lymphocyte-related ratios was less consistent, with significance observed only in univariate analyses. This finding is biologically plausible, as a high MLR often reflects an abundance of myeloid-derived suppressor cells (MDSCs) and tumor-associated macrophages (TAMs), which are known to suppress T cell function and promote tumor progression through various mechanisms, including arginase metabolism and the production of immunosuppressive cytokines.[13] The negative correlation we observed between MLR and T cell infiltration provides further mechanistic support for this paradigm.

Table 3 Univariate Analysis of PNI, LMR, PLR with DFS

Clinicopathological Characteristics	n	DFS (%)	χ2	P
Age (years)				
≤60	75	90.7	6.189	0.013
>60	23	91.3		
Sex				
Male	82	90.2	3.044	0.803
Female	16	93.8		
Lymphovascular Invasion (LVI)				
Negative	69	91.3	4.866	0.561
Positive	28	89.7		
Lymph node status				
Negative	91	93.4	10.249	0.001
Positive	7	57.1		
LMR				
≤2.38	27	100	7.596	0.006
>2.38	71	90.8		
PLR				
≤88.64	54	98.1	7.752	0.005
>88.64	44	81.8		
PNI				
≤41.6	25	72.0	14.247	<0.001
>41.6	73	97.3		

Table 4 Multivariate Analysis of LMR, PLR, PNI, Lymph Node Status with DFS

Clinicopathological Characteristics	β	SE	Wald	HR (95% CI)	P
LMR (≤2.38vs>2.38)	0.517	0.571	0.782	1.677 (0.356, 7.906)	0.377
PLR (≤88.64vs>88.64)	−1.697	0.558	10.332	0.183 (0.018, 1.920)	0.001
PNI (≤41.6vs>41.6)	1.820	0.601	5.478	6.172 (1.110, 34.329)	0.019
Lymph nodestatus (Negative vs Positive)	2.114	0.867	5.945	8.283 (1.514, 45.311)	0.015

Table 5 Association Between LMR Groups and Clinicopathological Characteristic

Clinicopathological Characteristics	High LMR Group (n=71)	Low LMR Group (n=27)	χ2	P
Age (years)				
≤60	59 (83.1)	16 (59.3)	2.084	0.149
>60	12 (16.9)	11 (40.7)		
Sex				
Male	59 (83.1)	23 (85.2)	0.062	0.803
Female	12 (16.9)	4 (14.8)		
Lymphovascular Invasion (LVI)				
Negative	49 (69.0)	20 (74.1)	0.240	0.624
Positive	22 (31.0)	7 (25.9)		
Lymph node status				
Negative	67 (94.4)	24 (88.9)	0.885	0.347
Positive	4 (5.6)	3 (11.1)		

https://doi.org/10.2147/JHC.S587532

Table 6 Association Between PLR Groups and Clinicopathological Characteristics

Clinicopathological Characteristics	High PLR Group (n=44)	Low PLR Group (n=54)	χ2	P
Age (years)				
≤60	31 (70.5)	44 (81.5)	1.641	0.200
>60	13 (29.5)	10 (18.5)		
Sex				
Male	37 (84.1)	45 (83.3)	0.010	0.920
Female	7 (15.9)	9 (16.7)		
Lymphovascular Invasion (LVI)				
Negative	29 (65.9)	40 (74.1)	0.776	0.378
Positive	15 (34.1)	14 (25.9)		
Lymph node status				
Negative	41 (93.2)	50 (92.6)	0.013	0.910
Positive	3 (6.8)	4 (7.4)		

Table 7 Association Between PNI Groups and Clinicopathological Characteristics

Clinicopathological Characteristics	High PNI Group (n=73)	Low PNI Group (n=25)	χ2	P
Age (years)				
≤60	55 (75.3)	20 (80.0)	0.225	0.635
>60	18 (24.7)	5 (20.0)		
Sex				
Male	59 (80.8)	23 (92.0)	1.703	0.192
Female	14 (19.2)	2 (8.0)		
Lymphovascular Invasion (LVI)				
Negative	53 (72.6)	16 (64.0)	0.661	0.416
Positive	20 (27.4)	9 (36.0)		
Lymph node status				
Negative	69 (94.5)	22 (88.0)	1.194	0.275
Positive	4 (5.5)	3 (12.0)		

Beyond the local microenvironment, our study highlights the significant prognostic power of preoperative peripheral blood indices. The Prognostic Nutritional Index (PNI) and Platelet-to-Lymphocyte Ratio (PLR) were identified as independent predictors of disease-free survival. PNI, which integrates albumin levels and lymphocyte count, is a marker of a patient's nutritional and immune status. A low PNI likely signifies a state of cancer-related cachexia and systemic immune incompetence, which compromises the host's ability to combat tumor recurrence post-resection.[14] The elevated PLR, on the other hand, may represent a pro-tumorigenic state where platelets facilitate metastatic spread and angiogenesis, coupled with relative lymphocytopenia, which diminishes immune surveillance.[15] It is noteworthy that in our cohort, the prognostic utility of PNI and PLR surpassed that of the more commonly studied Neutrophil-to-Lymphocyte Ratio (NLR), suggesting these indices may offer a more nuanced reflection of the host-tumor interaction in HCC.

The longitudinal perspective offered by our stage-based analysis reveals a dynamic co-evolution of the tumor and its immune context. The progressive decline in effector immune cells (T cells, NK cells) and the concurrent rise in immune checkpoint molecule expression from early to advanced stages depict a TIME that is progressively subdued and suppressed. This pattern illustrates a fundamental shift in the balance of power within the TIME, where immunosuppressive mechanisms eventually override anti-tumor immunity, facilitating immune escape and disease progression.[16] This observation underscores the clinical imperative for therapeutic intervention at earlier disease stages when the immune system is more competent and potentially responsive.

Collectively, our integrated analysis of the TIME and systemic inflammatory markers not only confirms known prognostic factors but also provides new insights into the coordinated nature of anti-tumor immunity and the differential utility of peripheral blood indices in HCC. These findings align with and extend the existing literature, offering a more comprehensive framework for risk stratification and potentially guiding future immunotherapy strategies.

However, Several limitations of this study should be acknowledged. First, the retrospective design may introduce inherent selection bias, and the findings warrant confirmation in prospective cohorts. Second, the prognostic value of the immune-related markers was assessed using data from a single cohort (TCGA) without external validation, limiting the generalizability of the results. Future studies with larger sample sizes and independent validation cohorts are needed to confirm these findings.

Conclusion

In conclusion, this study provides an integrated evaluation of both the local tumor immune microenvironment and systemic inflammatory markers in hepatocellular carcinoma, demonstrating that the coordinated interplay among adaptive immune cell subsets within the TIME, together with preoperative nutritional and inflammatory indices, collectively shapes patient prognosis. Our findings confirm the favorable prognostic role of $CD8^+$ T cells and reveal a broader collaborative network involving B cells and NK cells within immune-hot tumors, supporting a shift toward viewing the TIME as an integrated ecosystem. Peripheral blood markers, particularly PNI and PLR, emerged as independent predictors of postoperative recurrence, with prognostic utility surpassing that of NLR in our cohort. Furthermore, the stage-dependent erosion of effector immunity and the accumulation of immunosuppressive features underscore the importance of early therapeutic intervention. While these results are consistent with and extend the existing literature, they require validation in prospective, multi-center cohorts. Collectively, our findings offer a clinically relevant framework for risk stratification and highlight potential avenues for refining immunotherapy strategies in HCC.

Abbreviations

TIME, Tumor Immune Microenvironment; HCC, Hepatocellular carcinoma; HBV, Hepatitis B; HCV, Hepatitis C; DFS, Disease-free survival; OS, Overall survival; MDSCs, Myeloid-derived suppressor cells; TAMs, Tumor-associated macrophages; Tregs, Regulatory T cells; TNF-α, Tumor Necrosis Factor-alpha; NLR, Neutrophil-to-Lymphocyte Ratio; PLR, Platelet-to-Lymphocyte Ratio; LMR, Lymphocyte-to-Monocyte Ratio; PNI, Prognostic Nutritional Index; ROC, Receiver Operating Characteristic; NK, Natural Killer.

Data Sharing Statement

The datasets used and/or analysed during the current study are available from the corresponding author on reasonable request.

Ethics Approval and Consent to Participate

The study was performed in accordance with the Declaration of Helsinki and relevant guidelines and regulations. Study participants obtained ethical approval from the committee/institutional review board of the Xijing Hospital approved our study (Approval Number: KY20253406-1). The study was conducted in strict accordance with the STROBE guidelines; therefore, informed consent was waived. All patient information was de-identified during the study process to ensure strict confidentiality of patient data.

Consent for Publication

Publication was approved by all authors and by the responsible authorities where the work was carried out.

Author Contributions

All authors made a significant contribution to the work reported, whether that is in the conception, study design, execution, acquisition of data, analysis and interpretation, or in all these areas; took part in drafting, revising or critically reviewing the article; gave final approval of the version to be published; have agreed on the journal to which the article has been submitted; and agree to be accountable for all aspects of the work.

Funding

There is no funding to report.

Disclosure

The authors declare no conflicts of interest.

References

1. Sung H, Ferlay J, Siegel RL, et al. Global Cancer Statistics 2020: GLOBOCAN estimates of incidence and mortality worldwide for 36 cancers in 185 countries. *CA Cancer J Clin*. 2021;71(3):209–249. doi:10.3322/caac.21660
2. Llovet JM, Kelley RK, Villanueva A, et al. Hepatocellular Carcinoma. *Nat Rev Dis Primers*. 2021;7(1):6. doi:10.1038/s41572-020-00240-3
3. Ringelhan M, Pfister D, O'Connor T, et al. The immunology of hepatocellular carcinoma. *Nat Immunol*. 2018;19(3):222–232. doi:10.1038/s41590-018-0044-z
4. Grivennikov SI, Greten FR, Immunity KM. Inflammation, and Cancer. *Cell*. 2010;140(6):883–899. doi:10.1016/j.cell.2010.01.025
5. Binnewies M, Roberts EW, Kersten K, et al. Understanding the Tumor Immune Microenvironment (TIME) for Effective Therapy. *Nat Med*. 2018;24(5):541–550. doi:10.1038/s41591-018-0014-x
6. Kurebayashi Y, Ojima H, Tsujikawa H, et al. Landscape of immune microenvironment in hepatocellular carcinoma and its additional impact on histological and molecular classification. *Hepatology*. 2018;68(3):1025–1041. doi:10.1002/hep.29904
7. Zheng C, Zheng L, Yoo JK, et al. Landscape of infiltrating t cells in liver cancer revealed by single-cell sequencing. *Cell*. 2017;169(7):1342–1356. doi:10.1016/j.cell.2017.05.035
8. Bluestone JA. The 2025 nobel prize in physiology or medicine - a bridge to peripheral immune tolerance. *J Clin Invest*. 2025;135(23):e202216. doi:10.1172/JCI202216
9. Porta C, De Amici M, Quaglini S, et al. Circulating interleukin-6 as a tumor marker for hepatocellular carcinoma. *Ann Oncol*. 2014;25(2):353–358.
10. Liao R, Li DW, Du CY, et al. Combined preoperative crp and nlr levels as a predictor of prognosis in patients with hepatocellular carcinoma. *Cancer Manag Res*. 2018;10:3207–3214. doi:10.2147/CMAR.S160578
11. Wang D, Bai N, Hu X, et al. Preoperative inflammatory markers of nlr and plr as indicators of poor prognosis in resectable HCC. *PeerJ*. 2020;8:e8292. doi:10.7717/peerj.8292
12. Sun K, Chen S, Xu J, et al. The prognostic significance of the prognostic nutritional index in cancer: a systematic review and meta-analysis. *J Cancer Res Clin Oncol*. 2020;146(6):1537–1549.
13. Fridman WH, Pages F, Sautes-Fridman C, et al. The immune contexture in human tumours: impact on clinical outcome. *Nat Rev Cancer*. 2012;12(4):298–306. doi:10.1038/nrc3245
14. Veglia F, Sanseviero E, Gabrilovich DI. Myeloid-derived suppressor cells in the era of increasing myeloid cell diversity. *Nat Rev Immunol*. 2021;21(8):485–498. doi:10.1038/s41577-020-00490-y
15. Templeton AJ, Ace O, McNamara MG, et al. Prognostic role of platelet to lymphocyte ratio in solid tumors: a systematic review and meta-analysis. *Cancer Epidemiol Biomarkers Prev*. 2014;23(7):1204–1212. doi:10.1158/1055-9965.EPI-14-0146
16. Pinter M, Jain RK, Duda DG. The current landscape of immune checkpoint blockade in hepatocellular carcinoma. *Cancer J*. 2021;27(3):219–227.